Paleoceanography and Paleoclimatology

Supporting Information for

1050 years of hurricane strikes on Long Island in The Bahamas

[E. J. Wallace[1], J. P. Donnelly[2], P. J. van Hengstum[3,4], T. S. Winkler[4], K. McKeon[5,2], D. MacDonald[5], N. E. d'Entremont[2], R. M. Sullivan[4], J. D. Woodruff[5], A. D. Hawkes[6], C. Maio[7]]

[[1]Massachusetts Institute of Technology/Woods Hole Oceanographic Institution Joint Program in Oceanography, Woods Hole, Massachusetts 02543, USA; [2]Department of Geology and Geophysics, Woods Hole Oceanographic Institution, Woods Hole, Massachusetts 02543, USA; [3]Department of Marine Sciences, Texas A&M University at Galveston, Galveston, Texas, 77554, USA; [4]Department of Oceanography, Texas A&M University, College Station, Texas, 77840, USA; [5]Department of Geosciences, University of Massachusetts Amherst, Amherst, Massachusetts, 01003, USA; [6]Department of Earth and Ocean Sciences, Center for Marine Sciences, University of North Carolina Wilmington, Wilmington, North Carolina, 28403-5944, USA; [7]Department of Geosciences, University of Alaska Fairbanks, Fairbanks, Alaska, 99775, USA]

Contents of this file

Introduction

The supporting information includes supplementary figures and tables that are referred to in the main text.

1. Methods for CTD data collection

In April 2016, we collected conductivity temperature depth (CTD) casts (Figure S1) from Long Island Blue Hole (LIBH) using a YSI Castaway CTD. In January 2017, we collected CTD data using the YSI EXO1 sonde. The EXO1 sonde collects, in addition to profiles of temperature and salinity, profiles of dissolved oxygen and pH. All sensors on the sonde were calibrated within 24 hours of data collection. The sonde sampled at two readings per second with a 2-3 second applied rapid averaging. We lowered the sonde into LIBH at a rate of ~1 cm/s. Estimated sensor accuracy is: temperature = ±0.01 °C, salinity = ±0.1 PSU, dissolved oxygen = ±0.01 mg/L, pH = ±0.01 pH units.

2. Tiltmeter data: Temperature and bottom current speed and direction

Monthly climatology: The tiltmeter recorded bottom current and temperature data from near Long Island blue hole for a little over one year (from January 5, 2017 to March 20, 2018). We measured temperature at 2-minute intervals. For the current speed and direction data, we used burst logging to save battery, with a burst interval of 2 minutes, a burst rate of 8 Hz, and a burst duration of 30 seconds. This means that the logger wakes up every 2 minutes and records data at 8 Hz for 30 seconds and then goes back to sleep for 1 minute and 30 seconds. This data is then post processed into 2-minute velocity and direction records. It captured data during distant storm conditions (Hurricane Irma and Hurricane Maria) and ambient conditions. A monthly climatology of current speed from 2017-2018 shows higher average current speed (~5.5 cm/s) for the winter months (January–April) and current direction predominantly to the southwest (Figure S11). Current direction and speed change moving into the remainder of the year (May-December). Average current speed is almost half that observed in the first four months of the year (~3 cm/s). Current direction is predominantly to the northwest in May through August. September through December is characterized by a bimodal distribution in current direction both to the northwest and southwest. Temperature readings in the shallow waters near the blue hole show increasing (decreasing) temperature from May to June (September to January). The bottom water temperature plateaus in the summer months with peak values close to 30°C. Wintertime temperatures are approximately 6°C cooler than summer (Figure S7a).

Temperature changes in September 2017: Ambient water temperatures in September oscillate each day between a low of 30.6°C at night and 32.6°C in the mid-afternoon (Figure S7b). During Hurricane Irma on September 7, 2017, water temperature near the blue hole dropped approximately 5°C in under 24 hours overpowering daily temperature oscillations. Over the week following the storm, temperatures rose back to pre-storm values (~31°C). The more distal passage of Hurricane Maria also affected temperatures near the hole to a lesser degree. Average temperatures dropped approximately 1°C on September 22 with peak daily temperatures at 30.1°C and daily lows around 28.6°C. This lasted for approximately 2 days as Maria passed to the northeast (September 23-24) before temperatures around the blue hole began to rise again.

3. Justification for unused radiocarbon results

We excluded five radiocarbon dates from the age model. Three of them were not chronologically consistent with all the other dating evidence. The other two excluded dates were post-bomb radiocarbon dates from 22 cm and 29 cm downcore (Figure 2 and Table S3). The post-bomb calibration curve allows us to estimate the age of these samples with less than one year of uncertainty. Both samples calibrated to the same year (1956 ± 1 CE). This uncertainty is too small given that it does not account for the residence time of the mangrove leaves on the landscape before they are transported into the blue hole. While both of the plant macrofossils may have died in 1956 CE, we cannot tell how many years passed before they were deposited in the blue hole, which is located about 0.5 km away from shore. Therefore, we expect that both samples are either 1956 or older, dependent how long they resided on the landscape before being transported into the blue hole. The fact that the second sample located 7 cm downcore from top sample (at 22 cm) dated to the same year provides evidence that this sort of phenomenon could be happening. If both plant samples were deposited in the blue hole immediately after they died, the second sample should have an older date than the sample closer to the core top. We choose to exclude these samples, because we think they force the age model through too small of an uncertainty range. However, both of these samples are consistent with the dating evidence provided by both the ^{210}Pb and pollen horizons (Figure 2).

4. Methods for Northeast Gulf, New England, and Bahamas sediment compilation

The sediment compilation for The Bahamas included events from the Long Island blue hole reconstruction, Abaco Island reconstruction (Thatchpoint Blue Hole (Winkler et al., 2020)) and South Andros Island reconstructions (AM5, AM4 and AM2 records (Wallace et al., 2019)). We also created compilations of paleohurricane records from New England and Northeast Gulf Coast. To allow for appropriate comparison with The Bahamas blue hole records, we only include previously published records in the New England and Northeast Gulf Coast compilations if they meet the following three criteria:

1) Each record must have at least multi-decadal resolution and extend back at least 500 years.
2) There must be clear criteria established in the paper for what is considered a storm event with clear attribution to modern tropical cyclones.
3) Each published record must provide enough information to create or replicate a well-dated Bayesian age model for estimating age uncertainties.

For the Northeast Gulf Coast compilation, we create a High Threshold (HT) compilation as specified in the publications which include Category 3 and above events. The Northeast Gulf Coast HT compilation includes work from Apalachee Bay (Spring Creek Pond (Brandon et al., 2013), Mullet Pond (Lane et al., 2011)) and Choctawhatchee Bay (Basin Bayou (Rodysill et al., 2020)). The New England compilation includes records from Salt Pond (Donnelly et al., 2015) and Mattapoisett Marsh (Boldt et al., 2010).

We recreated the age models for each of these studies using BACON software (Blaauw & Christen, 2011). To form each region/island's composite, we made efforts to

remove redundant counts of the same event among multiple contributing records. If multiple events on an island fell within age model uncertainties of each other, they were consolidated into single assumed hurricane strikes. We did this because many records from the same island/region capture many of the same historical landfalling hurricane events (see Wallace et al., 2019). When several events from one site fell within age model uncertainties of an event from another site, we only consolidate the event that is closest in median age to that of the event from the second site. Figure S12 shows the median age of the events included in the Apalachee Bay, Choctawhatchee Bay, New England, Andros, Abaco, and Long Island-wide composites.

Having consolidated redundant events, we create age probability distributions functions (pdfs) for each event in our region/island composites between 900-2016 CE. Each individual distribution sums to one and provides an estimate of how probable it is that each event happened in any given year within the age uncertainties. Many of these events' age pdfs overlap. To create the island/region-wide composites, we summed all the overlapping age pdf values for each island/region. To create our age distributions, we sampled 1000 different age ensembles from our Bayesian age models. For region/island-wide composites where we have multiple different records each with their own independent age model contributing to the compilation, we used the age model from the record with the smallest age uncertainties for each event. In the case of Andros, this was always AM4. For New England and Apalachee Bay, the age model used for each event varied. Figure S12 colors the events according to which age model we used to create its pdf.

We formed the final composites for The Bahamas, New England, and Northeast Gulf Coast by summing up all the contributing composites shown in Figure S12. Confidence intervals around this estimate were calculated as the spread among the different contributing island/region-wide composites in each year. This full compilation unsmoothed is shown in Figure S13.

References

Appleby, P. G. (2001). Chronostratigraphic Techniques in Recent Sediments. In W. M. Last & J. P. Smol (Eds.), *Tracking Environmental Change Using Lake Sediments: Volume 2: Physical and Geochemical Methods* (pp. 171–202). Kluwer Academic Publishers.

Appleby, P. G., & Oldfield, F. (1978). The Calculation of Lead-210 dates assuming a constant rate of supply of unsupported 210-Pb to the sediment. *Catena*, *5*, 1–8.

Blaauw, M., & Christen, J. A. (2011). Flexible paleoclimate age-depth models using an autoregressive gamma process. *Bayesian Analysis*, *6*(3), 457–474. https://doi.org/10.1214/11-BA618

Boldt, K. V., Lane, P., Woodruff, J. D., & Donnelly, J. P. (2010). Calibrating a sedimentary record of overwash from Southeastern New England using modeled historic hurricane surges. *Marine Geology*, *275*(1–4), 127–139. https://doi.org/10.1016/j.margeo.2010.05.002

Brandon, C. M., Woodruff, J. D., Lane, D. P., & Donnelly, J. P. (2013). Tropical cyclone wind speed constraints from resultant storm surge deposition: A 2500 year reconstruction of hurricane activity from St. Marks, FL. *Geochemistry, Geophysics, Geosystems*, *14*(8),

2993–3008. https://doi.org/10.1002/ggge.20217
Donnelly, J. P., Hawkes, A. D., Lane, P., Macdonald, D., Shuman, B. N., Toomey, M. R., Van Hengstum, P. J., & Woodruff, J. D. (2015). Climate forcing of unprecedented intense-hurricane activity in the last 2000 years. *Earth's Future*, *3*(2), 49–65. https://doi.org/10.1002/2014EF000274
Lane, P., Donnelly, J. P., Woodruff, J. D., & Hawkes, A. D. (2011). A decadally-resolved paleohurricane record archived in the late Holocene sediments of a Florida sinkhole. *Marine Geology*, *287*(1–4), 14–30. https://doi.org/10.1016/j.margeo.2011.07.001
Rodysill, J., Donnelly, J. P., Sullivan, R. M., Lane, P. D., Toomey, M. R., Woodruff, J. D., Hawkes, A. D., Macdonald, D., D'Entrement, N., McKeon, K., Wallace, E. J., & Van Hengstum, P. J. (2020). Historically unprecedented Northern Gulf of Mexico hurricane activity from 650 to 1250 CE. *Scientific Reports*, *10*, 1–17. https://doi.org/10.1038/s41598-020-75874-0
Wallace, E. J., Donnelly, J. P., van Hengstum, P. J., Wiman, C., Sullivan, R. M., Winkler, T. S., D'Entrement, N. E., Toomey, M. R., & Albury, N. A. (2019). Intense hurricane activity over the past 1500 years at South Andros Island, The Bahamas. *Paleoceanography and Paleoclimatology*, *34*(11), 1761–1783. https://doi.org/10.1029/2019PA003665
Winkler, T. S., Van Hengstum, P. J., Donnelly, J. P., Wallace, E. J., Sullivan, R. M., Macdonald, D., & Albury, N. A. (2020). Revising evidence of hurricane strikes on Abaco Island (The Bahamas) over the last 680 years. *Scientific Reports*, *10*. https://doi.org/https://www.nature.com/articles/s41598-020-73132-x

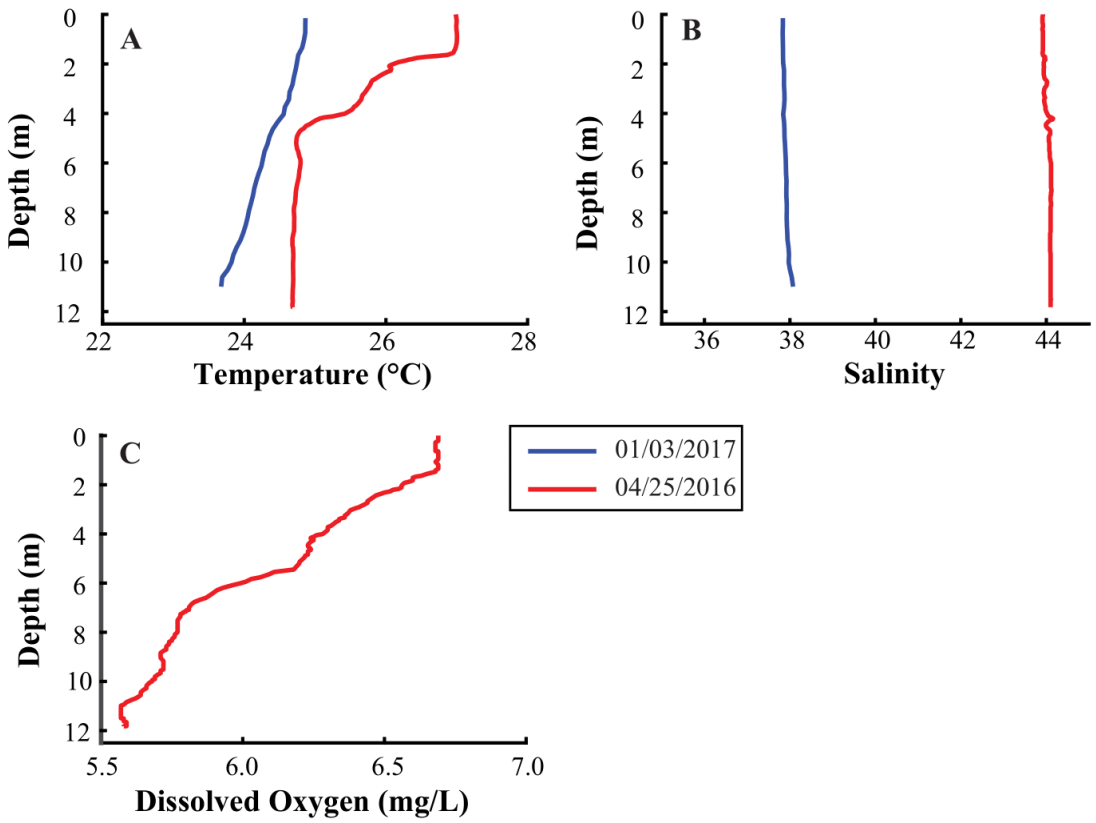

Figure S1. Temperature (A), salinity (B) and optical dissolved oxygen (C) in the Long Island blue hole (LIBH). Profiles from April 2016 (red) were collected using a YSI EXO1 sonde and the profiles from January 2017 (blue) were collected using a YSI Castaway CTD. There are no dissolved oxygen values for January because the YSI Castaway CTD does not measure dissolved oxygen.

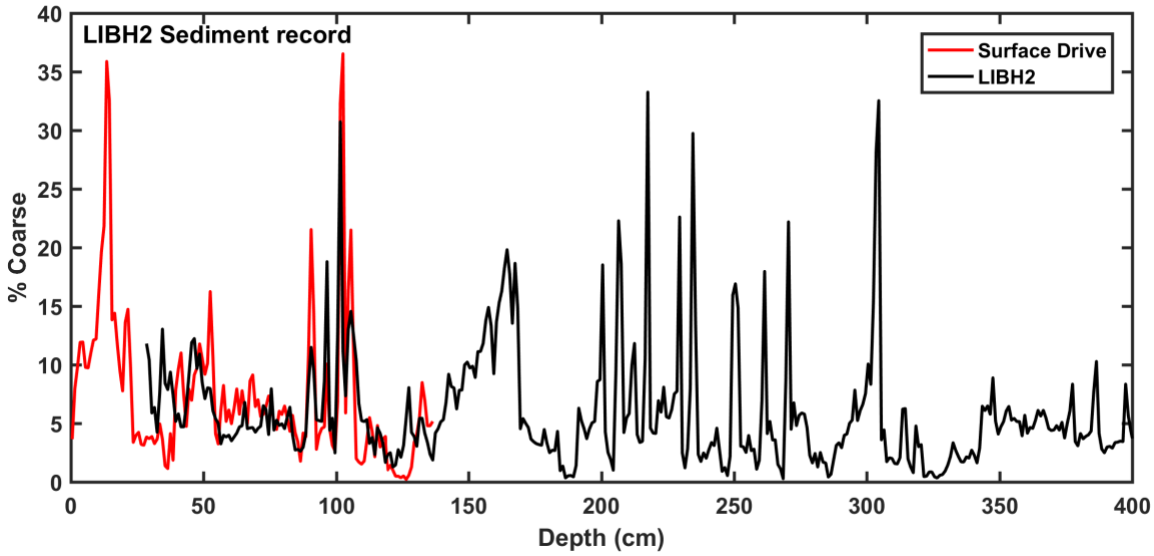

Figure S2. Percent sand fraction (> 63 μm) vs depth in core (cm) for the polycarbonate surface drive in red and LIBH2 (three-inch aluminum 12 m drive) in black. The figure shows the determined overlap between the two drives. Note LIBH2 (black) did not capture the sediment water interface.

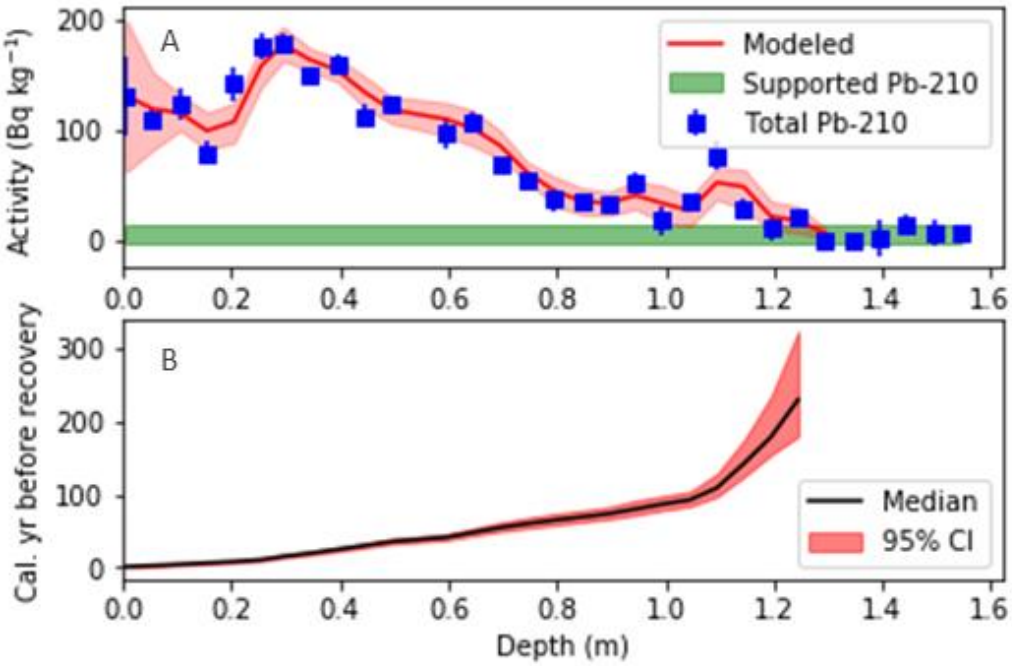

Figure S3. (**A)** Total (blue) and supported (green) Lead-210 activity with depth in the LIBH surface drive measured using Canberra GL2020RS low-energy Germanium gamma well detectors. Predicted Lead-210 values calculated using the Constant Rate of Supply (CRS) model (Appleby, 2001; Appleby & Oldfield, 1978) are shown in red. (**B**) Age (year before 2016, i.e. recovery) with depth in the top 125 cm of LIBH calculated using the CRS model. 95% confidence intervals are shown in red. The ^{210}Pb intercept of supported and total activity at 110 cm was dated to 1906 ± 10 CE.

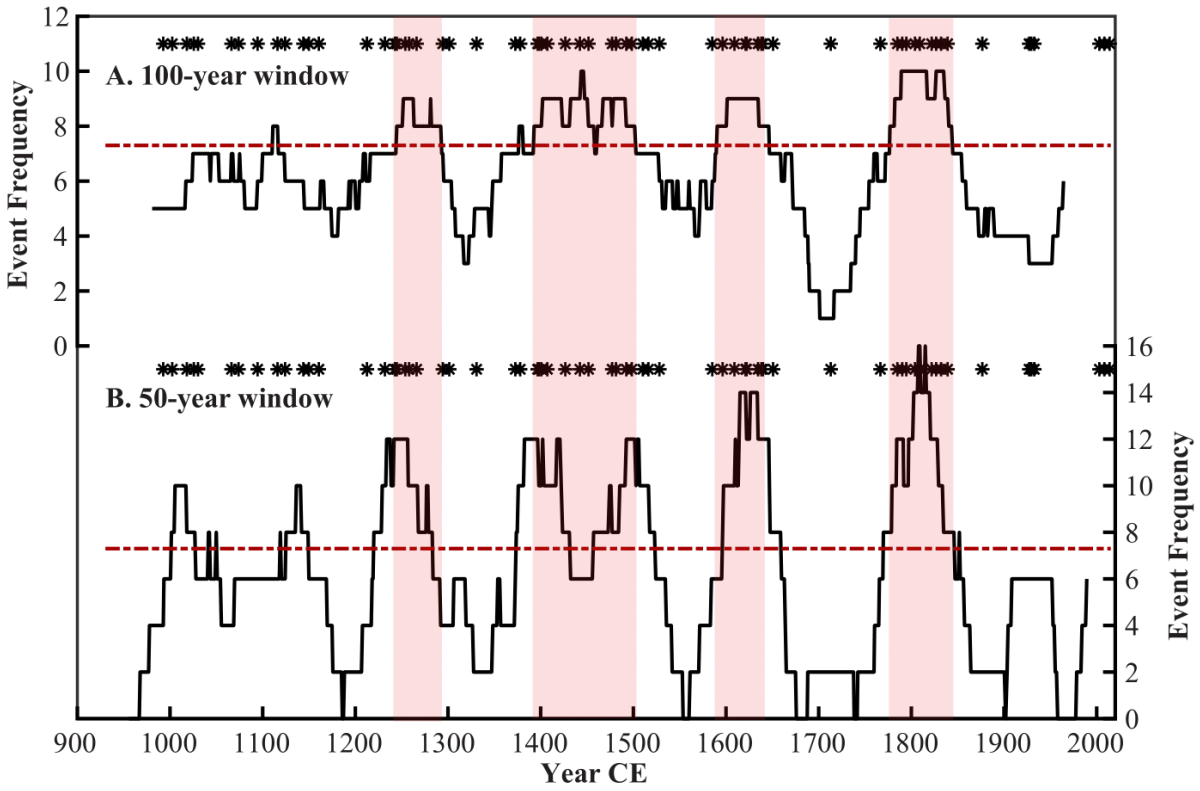

Figure S4. Event frequency per century for LIBH2 (black) with a 100-year sliding window (**A**) and a 50-year sliding window (**B**). The dashed red line is the regional cutoff for active intervals (7.3 events/century). Active intervals are shaded in red and indicate time periods when the event frequency is above the regional cutoff for the 100-year window event frequency. The median timing of each event is plotted as a black star above each panel. The timing of active intervals does not change dramatically if we use the 50-year window frequency versus the 100-year.

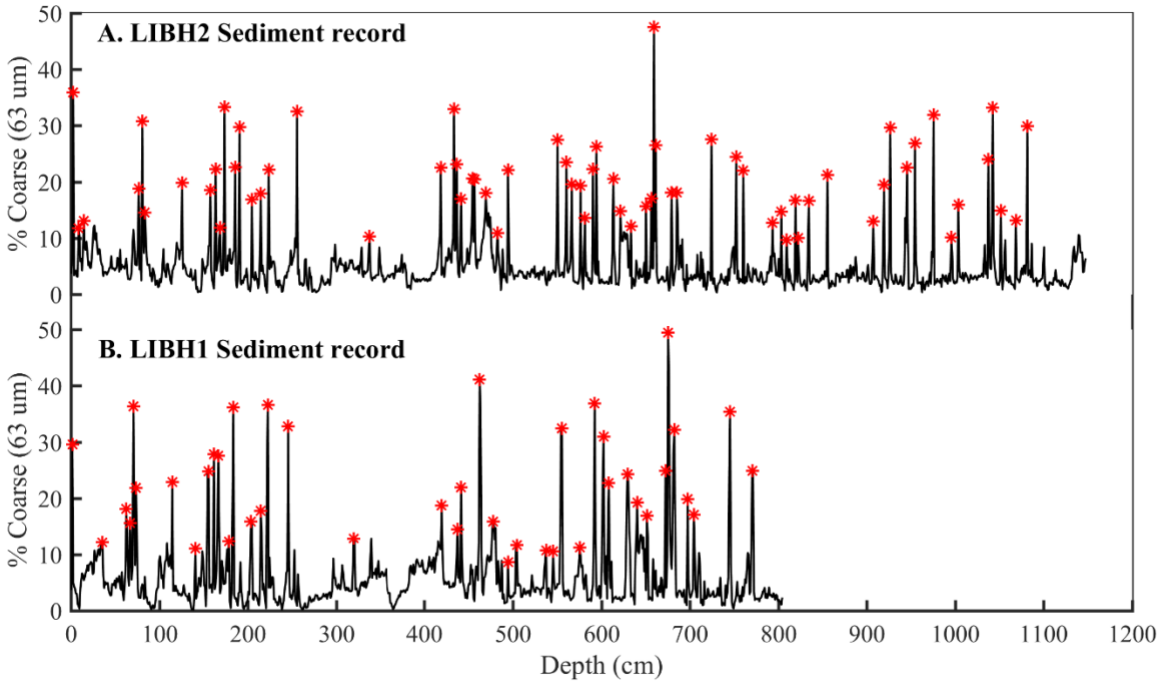

Figure S5. Percent sand fraction (>63 μm) vs. depth in core (black) from LIBH2 (A) and LIBH1 (**B**). Events beds in each core are denoted by a red star. Most of the event beds from LIBH2 correspond to an equivalent deposit in LIBH1. There are 45 events in the top 800 cm of LIBH2 and 42 events in the entirety of LIBH1.

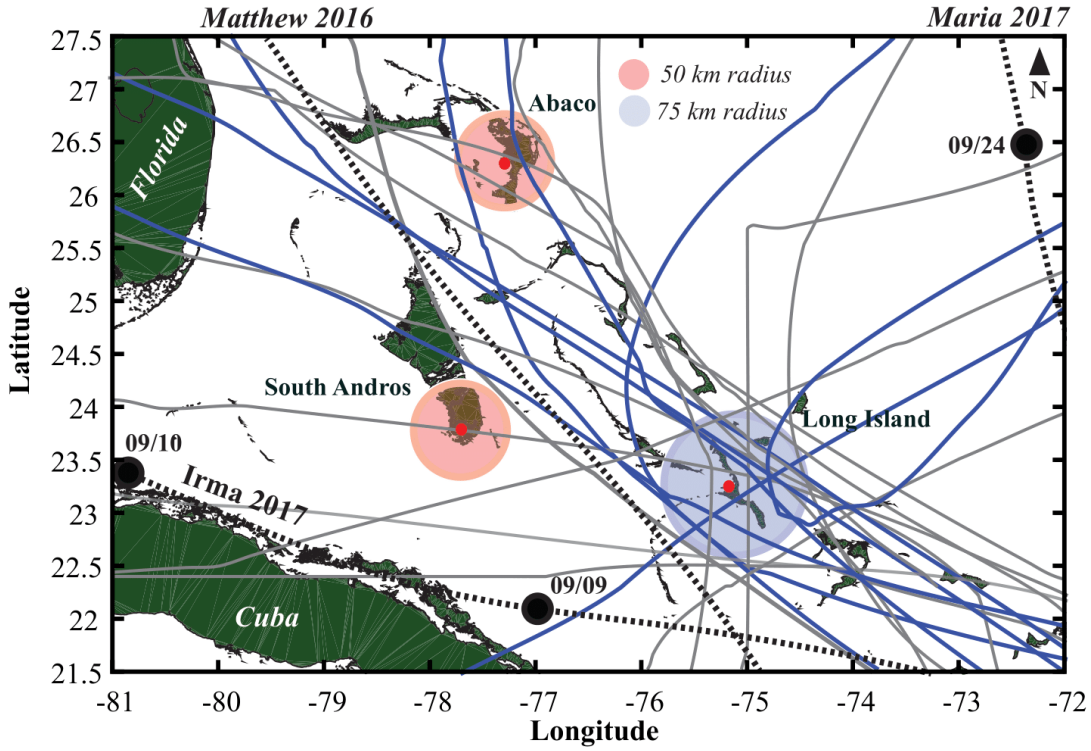

Figure S6: Map showing 50 km radii (red) around Thatchpoint Blue Hole on Abaco Island (Winkler et al., 2020) and the AM4 blue hole on South Andros Island (Wallace et al., 2019) and a 75 km radius around Long Island blue hole (blue). Red dots indicate the location of each paleohurricane site. Historical hurricane tracks (Category 1 and above from 1850-2016) passing within 100 km of Long Island are plotted in grey. Five of these storms and one of these storms go on to hit Thatchpoint and AM4, respectively. The blue tracks indicate the modern storms that left deposits in the Long Island blue hole. The dashed black lines show storms that passed near Long Island after 2015. Daily markers are placed on Hurricane Irma's and Maria's tracks.

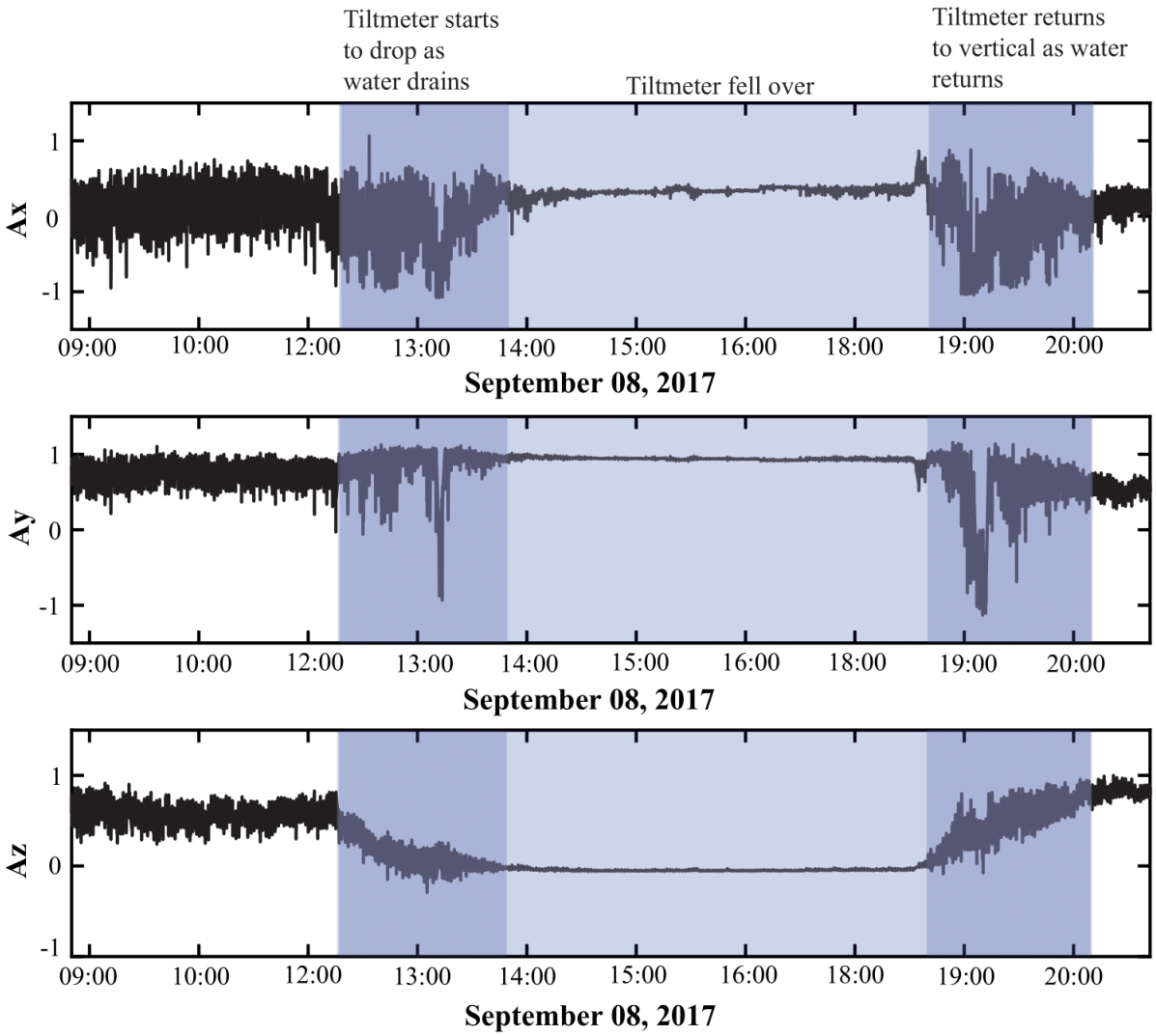

Figure S7. Raw accelerometer data during Hurricane Irma in 2017 measured on a Lowell Instruments LLC Tilt Current Meter (TCM). The noise prior to noon on September 8th shows the tiltmeter moving in the water. From approximately 12:00 to 14:00, Az panel shows the tiltmeter falling over. The lack of noise from ~14:00 to 19:00 indicates that the sensor was lying flat on the bank. The water returns at 19:00.

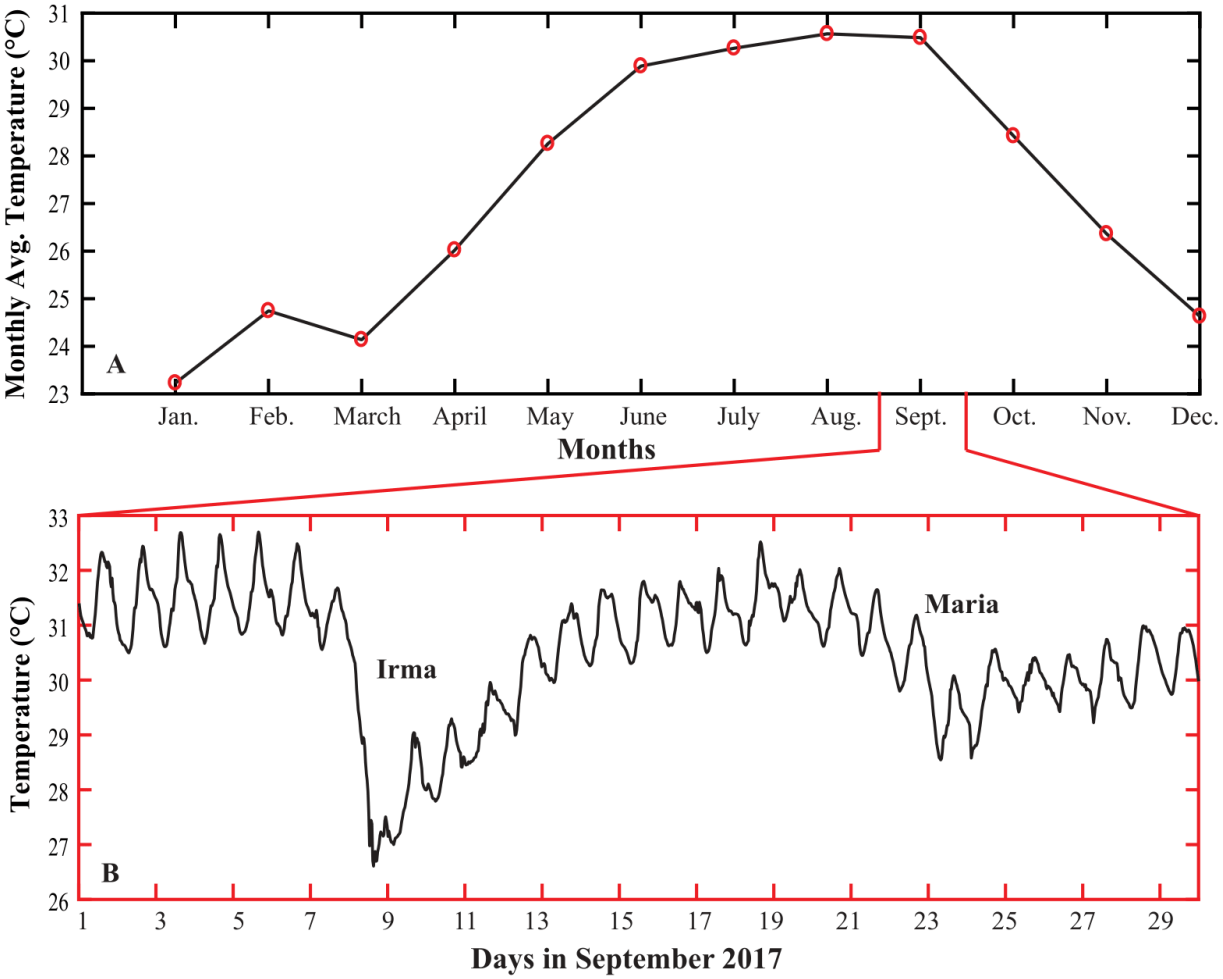

Figure S8. Monthly average temperature for the bank near Long Island blue hole in 2017 (**A**). Bottom water temperature in September 2017 (**B**). There is a clear drop in temperature on the bank during the distant passage of Hurricanes Irma and Maria. All data was taken from a Lowell Instruments LLC Tilt Current Meter (TCM).

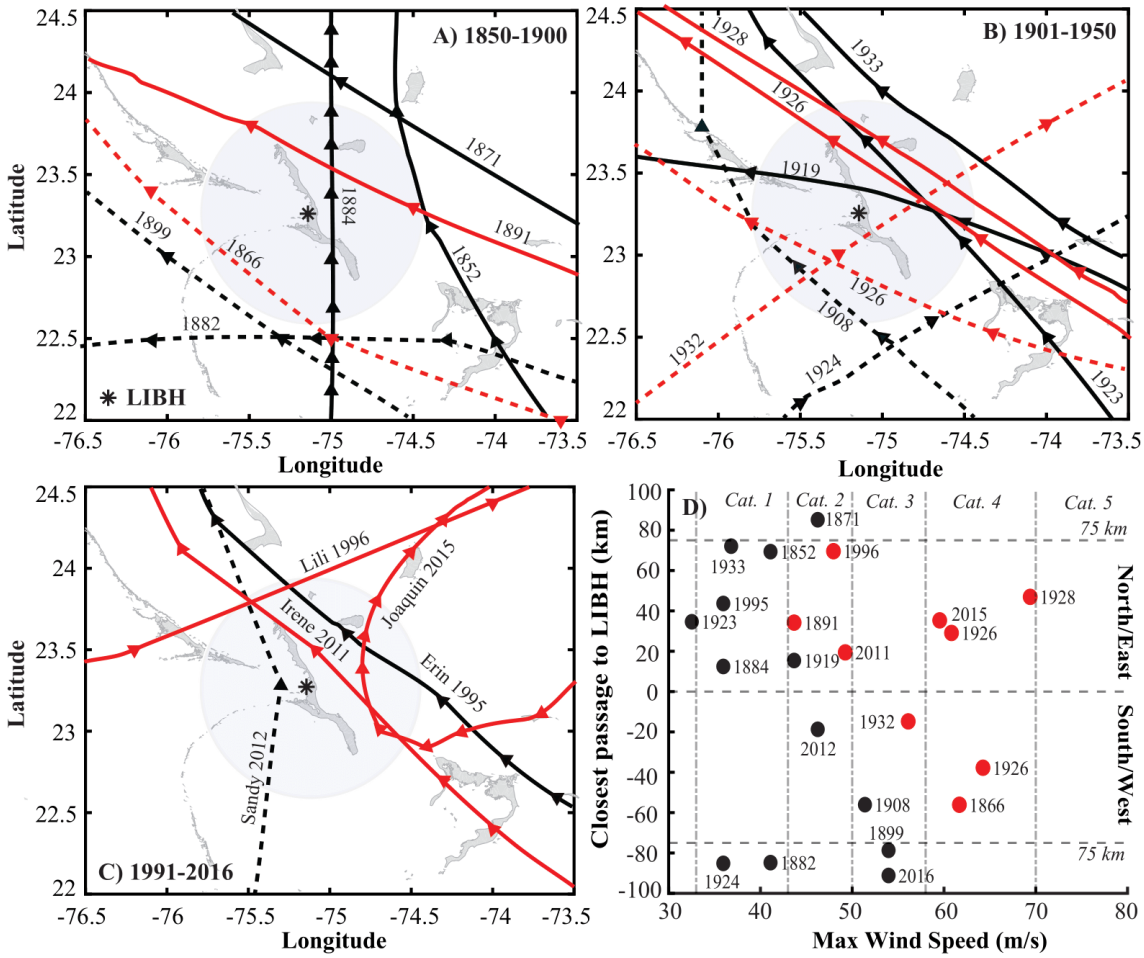

Figure S9. Historical hurricane tracks passing within 100 km of the Long Island blue hole (N 23.265°, W 75.117°) from 1850-1900 CE (**A**), 1901-1950 CE (**B**), and 1991-2016 CE (**C**). The arrows indicate 6 hourly points along each track and point in the direction of forward motion for each storm. Dashed tracks indicate storms that passed closest to LIBH to the west or south and solid tracks indicate storms that moved north or east of the site at closest passage. LIBH's location is denoted by the black star with a grey circle showing a 75 km radius around the site. (**D**) Historical hurricanes plotted as the distance of closest passage from LIBH as a function of their max sustained winds at that point. Red dots indicate the storms that left deposits in the blue hole. A storm's distance to LIBH is plotted as positive value if the storm's point of closest passage is to the north or east of LIBH and negative to the west or south of LIBH.

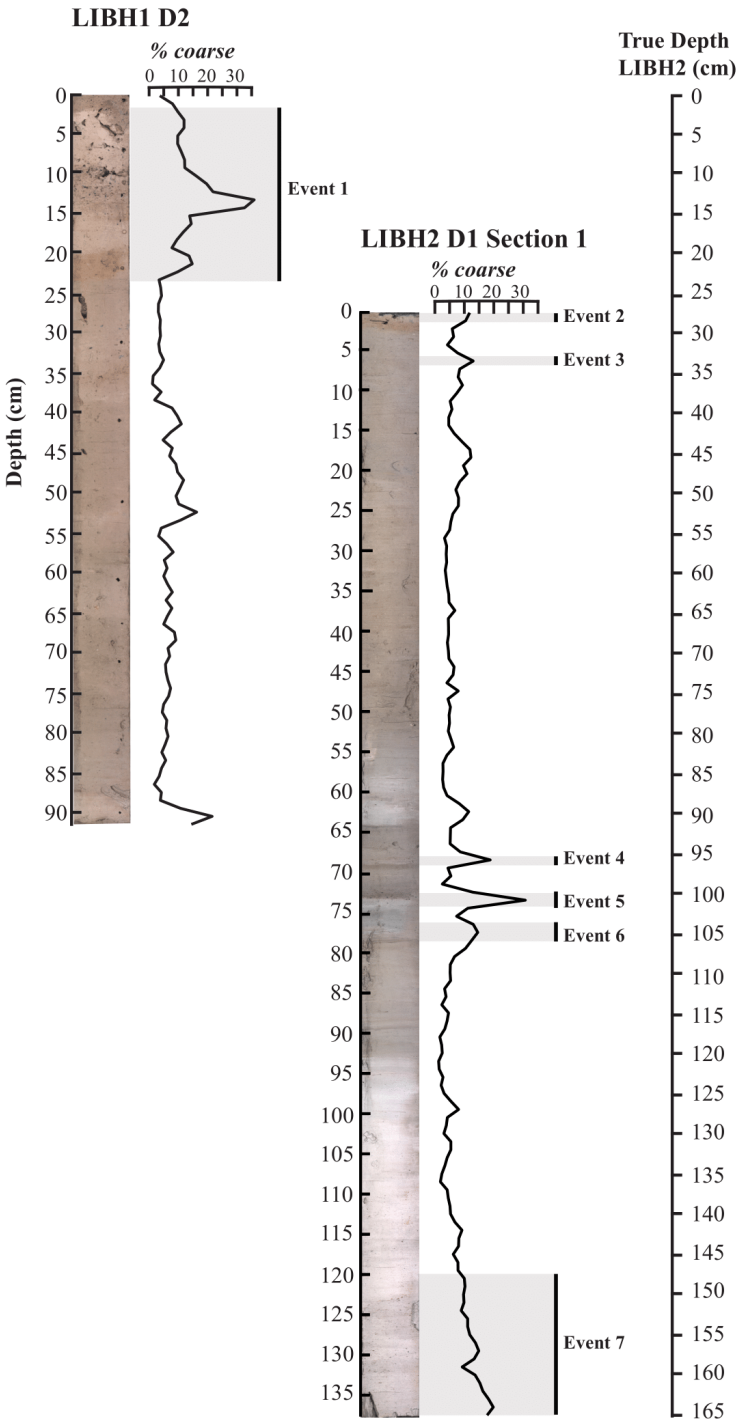

Figure S10. Pinpointing the overlap point between the first section of the Long Island surface drive (LIBH1 D2) and the first section of the longer drive (LIBH2 D1). The longer drive did not capture the sediment-water interface or the first event bed. Optical images from the ITRAX X-ray fluorescence scanner and coarse fraction (>63 um) data were used to choose the overlap points. Gray shaded vertical black bars with event labels indicate denote the thickness of event beds identified. Visual cues for event beds included: lighter colored sediments, visibly coarser grains, and higher concentrations of organics.

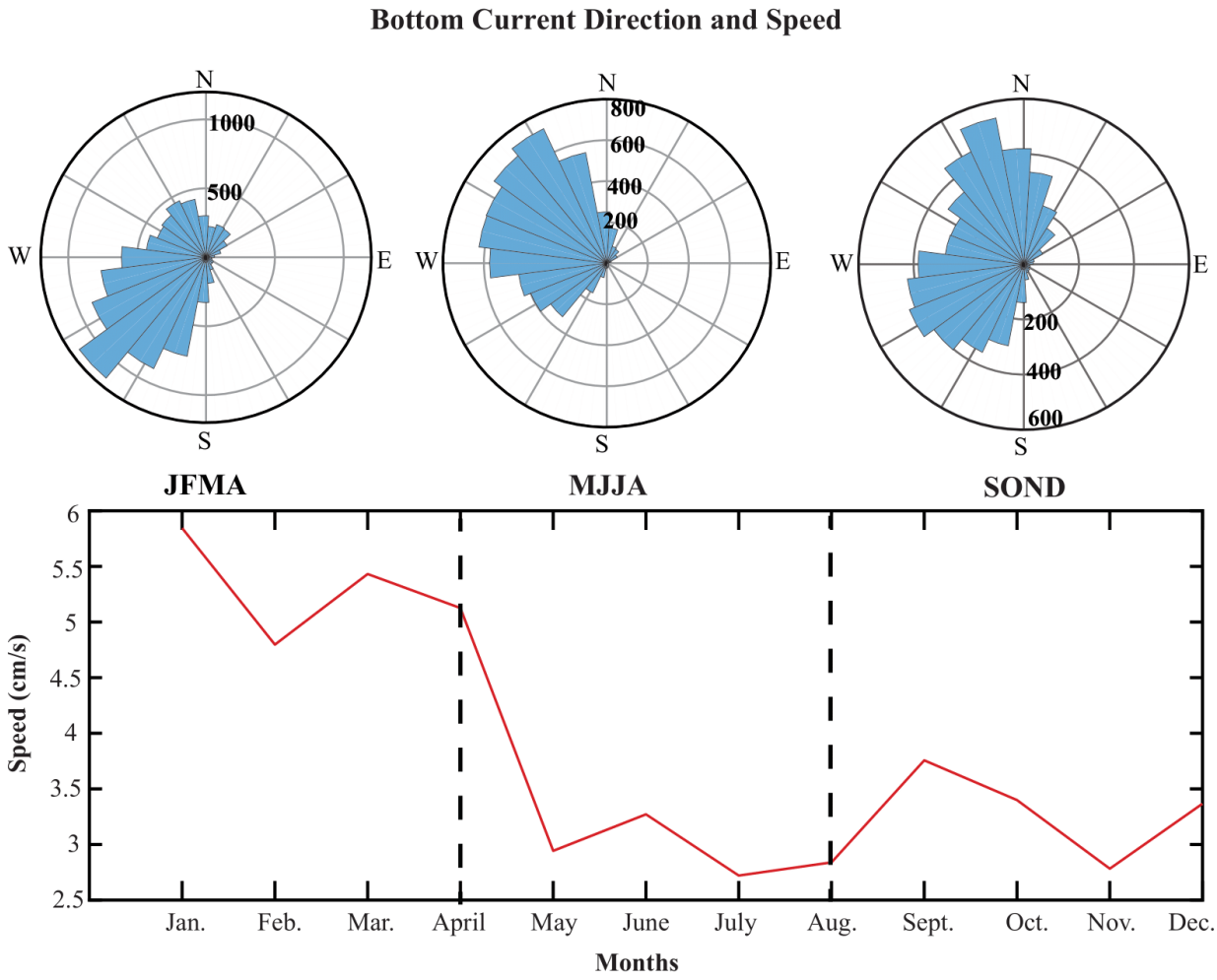

Figure S11. Monthly climatology of wave conditions near LIBH in 2017. We show rose plots of current direction in January-April (JFMA), May- August (MJJA), and September-December (SOND). Average bottom current speeds are shown for each month of the year. All data was taken from a Lowell Instruments LLC Tilt Current Meter (TCM).

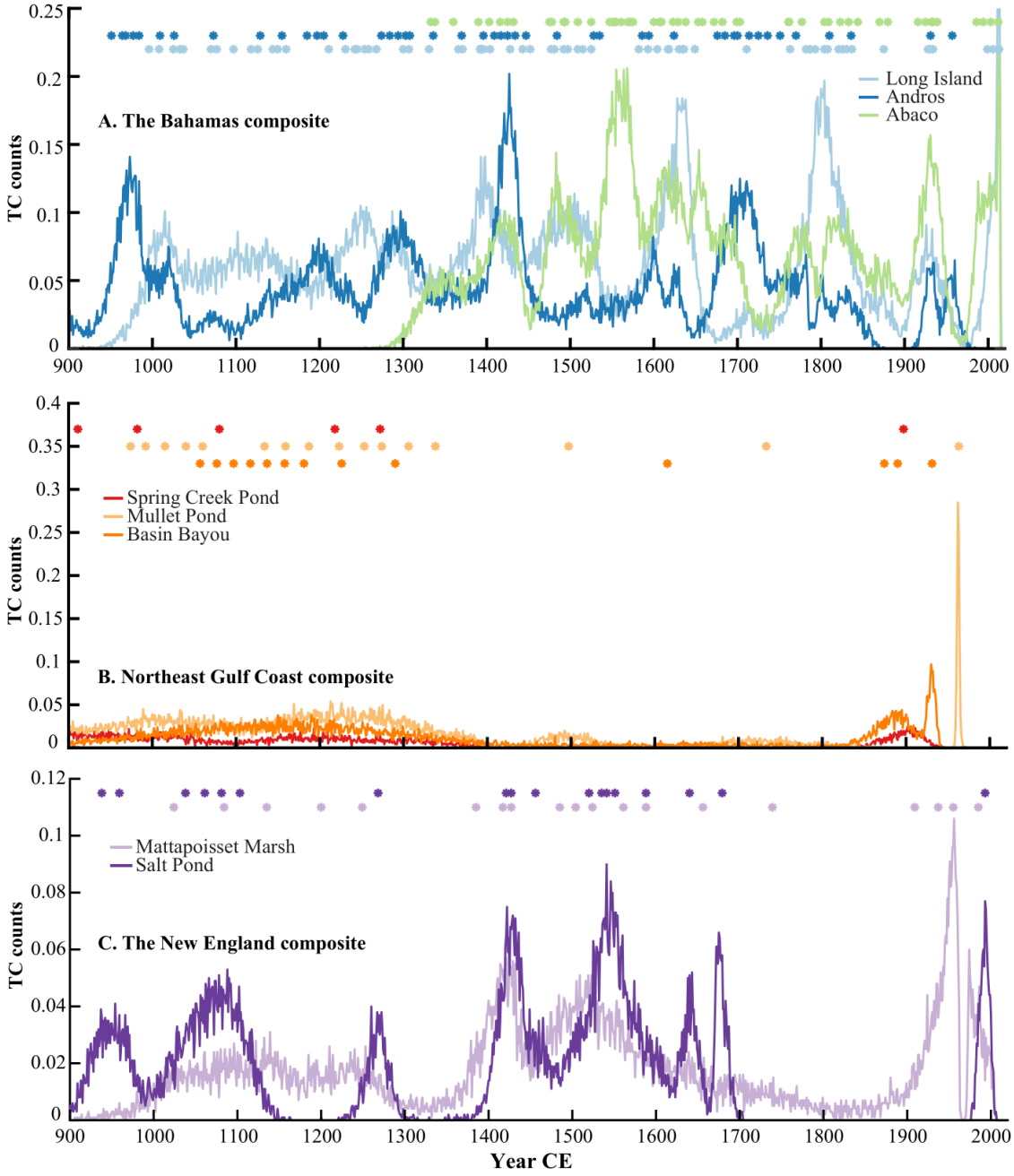

Figure S12. Components of regional compilations of hurricane counts from 900-2016 CE for the (**A**) The Bahamas: Abaco (light green), Andros (dark blue), and Long Island (light blue), (**B**) Northeast Gulf Coast (≥ Category 3): Spring Creek Pond (Brandon et al., 2013) (red), Mullet Pond (Lane et al., 2011) (light orange), and Basin Bayou (Rodysill et al., 2020 (dark orange), and (**C**) New England: Salt Pond (Donnelly et al., 2015) (purple) and Mattapoisett Marsh (Boldt et al., 2010) (lavender). Abaco includes events from Thatchpoint Blue Hole (Winkler et al., 2020). Andros includes events from the AM5, AM4 and AM2 records (Wallace et al., 2019). The dots at the top of each panel indicate the median age of each event used in the compilation. The compilations are the sum of the age probability distributions of each of these events.

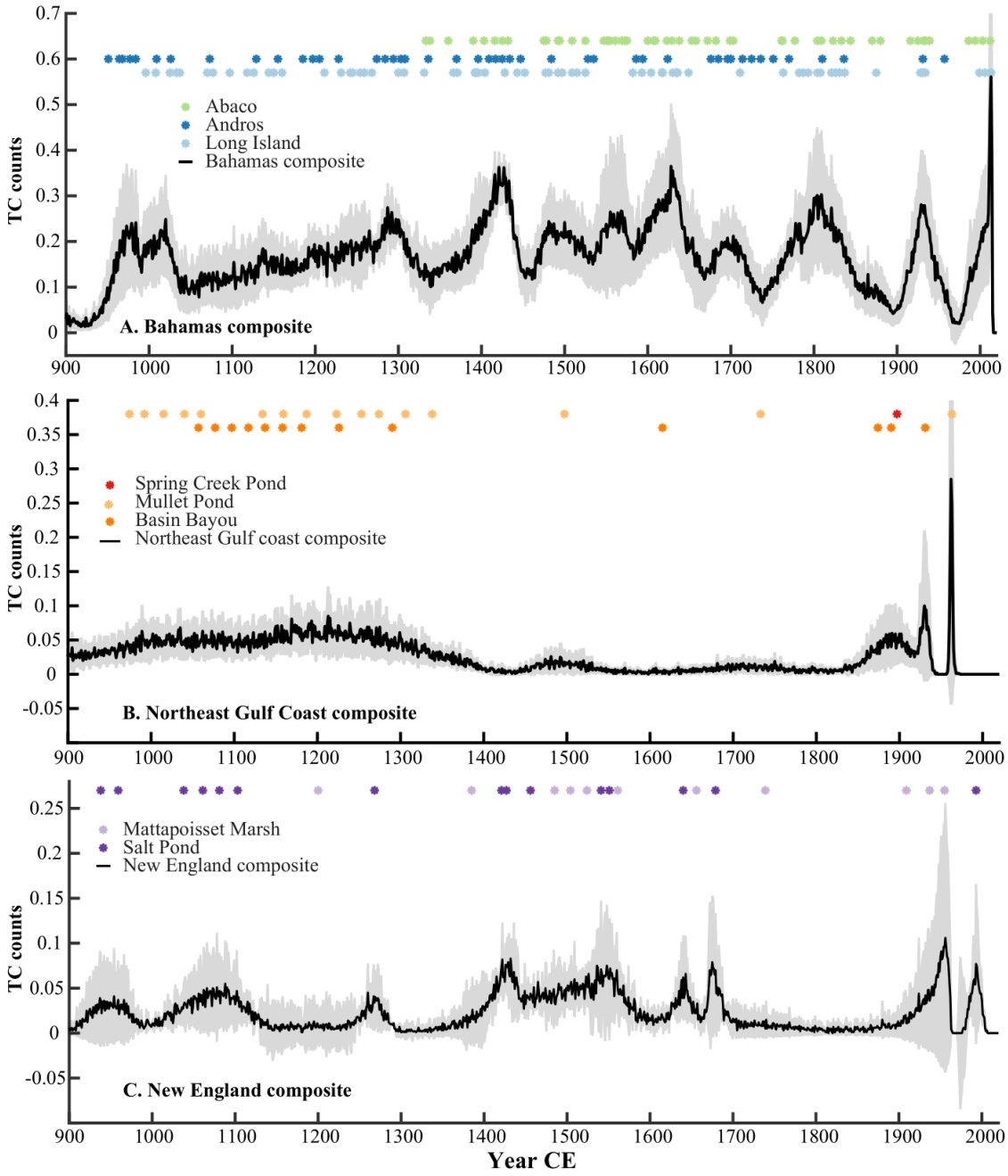

Figure S13. The Bahamas paleohurricane compilation (**A**), Northeast Gulf Coast paleohurricane compilation (**B**), and New England paleohurricane compilation (**C**) generated by summing the time series in Figure S12A, S12B, and S12C, respectively. Standard errors are shaded in grey around each compilations and are calculated as the spread among the estimates in Figure S12. The dots at the top of each panel indicate the median age of each event used in the compilation.

Table S1. Pollen smear slide data from LIBH2. This table includes identified taxa and interpretations of the environment and level of disturbance in each sample. Pollen taxa and opaque spherules are listed in order of dominance. The final column includes the dates (in year CE) and uncertainties included in the LIBH age model from these slides.

Core	Depth (cm)	Taxa	Environment	Disturbance	Year CE
LIBH2 D1	286.5	*Jacquemontia*, *Cordia*, Leguminosae, *Buxus*, Combretaceae, and Arecaceae	Dry tropical hardwood forest dominated by diverse woody vegetation and some palms	Not evident	
LIBH2 D1	233.5	*Caesalpinia*, *Swietenia* (mahogany), *Jacquemontia*, *Buxus*, Rubiaceae, *Typha*, and Asteraceae (short spine)	Dry tropical hardwood forest dominated by diverse woody vegetation	Slightly evident	
LIBH2 D1	193.5	*Jacquemontia*, Polygonaceae, *Typha*, Arecaceae, *Caesalpinia*, Asteraceae (short spine), Asteraceae (long spine), and *Ambrosia*	Dry tropical hardwood forest including some palms with agricultural disturbance	Very evident	1795 +/- 10
LIBH2 D1	181.5	Leguminosae, Malpighiaceae, *Spondias* (hog plum - from cultivation) , *Conyza*, *Ambrosia*, Asteraceae (short spine), Asteraceae (long spine), and *Iva*	Dry tropical hardwood forest with agricultural disturbance	Very evident	
LIBH2 D1	140.5	*Jacquemontia*, Malpighiaceae, *Chamaecrista lineata*, *Ipomoea*, Euphorbiaceae, and Leguminosae	Dry tropical hardwood forest	Not evident	
LIBH2 D1	128.5	*Jacquemontia*, *Picrodendron*, *Caesalpinia*, and *Swietenia*	Dry tropical hardwood forest	Not evident	
LIBH2 D1	98.5	*Acacia*, *Bauhinia* (non-native), Rubiaceae, Leguminosae, Euphorbiaceae, *Coccothrinax*, *Jacquemontia*, *Typha*, *Cordia*, *Ambrosia*, *Iva*, *Conyza*, and Agavaceae (c.f. *Agave sisalana*)	Scattered Dry tropical hardwood forest with some palms and sisal cultivation	Very evident	1905 +/- 15
LIBH2 D1	62.5	*Acacia*, *Jacquemontia*, Rubiaceae, *Ambrosia*, and *Conyza*	Dry tropical hardwood forest possibly minor disturbance	Slightly evident	
LIBH2 D1	40.5	Rubiaceae, *Jacquemontia*, Leguminosae, Opaque spherules, *Metopium*, , *Typha*, *Conyza*, and *Spondias* (hog plum - from cultivation)	Dry tropical forest with small clearings. More widespread use of automobiles, and possibly diesel generators, motorized boats, and tractors.	Slightly evident	
LIBH2 D1	18.5	*Jacquemontia*, Leguminosae, *Metopium*, Rubiaceae, Arecaceae, *Swietenia*, Passifloraceae, Cyperaceae, Opaque spherules	Dry tropical forest with some palms, with less fossil fuel combustion. Potentially reflecting the loss of farmers and farm sites.	Not evident	1980 +/- 20

Table S2. Radiocarbon results from leaf and plant matter in LIBH2.

Core	Laboratory Number	Core depth (cm)	Material dated	Conventional ^{14}C age	Error	F Modern	F Modern error	D13C
LIBH2 D1	OS-146534	118.5	Plant/Wood	200	20	0.9753	0.0023	-27.31
LIBH2 D1	OS-127198	174	Plant/Wood	145	20	0.9820	0.0026	-24.3
LIBH2 D1	OS-130637	197	Plant/Wood	190	15	0.9766	0.0021	-24.86
LIBH2 D1	OS-143921	243	Plant/Wood	360	85	0.9560	0.0099	-25.17
LIBH2 D1	OS-130782	362	Plant/Wood	115	40	0.9856	0.0052	-25.94
LIBH2 D1	OS-127824	413.5	Plant/Wood	290	20	0.96440	0.00230	-25.94
LIBH2 D1	OS-127197	517.5	Plant/Wood	310	20	0.9622	0.0022	-26.46
LIBH2 D1	OS-127301	619.5	Plant/Wood	585	15	0.92950	0.00170	-25.86
LIBH2 D1	OS-127196	707	Plant/Wood	650	15	0.9222	0.0020	-28.13
LIBH2 D1	OS-130781	870	Plant/Wood	900	30	0.8940	0.0038	-25.23
LIBH2 D1	OS-127194	979	Plant/Wood	995	15	0.88370	0.00190	-26.94

Table S3. Unused Radiocarbon results from leaf and plant matter in LIBH2 and LIBH1.

Core	Laboratory Number	Core depth (cm)	Material dated	Conventional ^{14}C age	Error	F Modern	F Modern error	D13C
LIBH2 D1	OS-146535	19	Plant/Wood	-6	0.5	1.0272	0.0021	-26.83
LIBH2 D2	OS-144104	26.5	Plant/Wood	-6.15	1	1.0378	0.0024	-27.04
LIBH2 D1	OS-127838	246	Plant/Wood	340	15	0.95840	0.00200	-26.03
LIBH2 D1	OS-127195	838	Plant/Wood	1,410	15	0.8388	0.0017	-7.68
LIBH1 D1	OS-144130	399.5	Plant/Wood	1,260	110	0.8544	0.0112	Not measured

Table S4: Modern hurricane event attribution for the LIBH record. This table lists the age range and median age of the first seven event beds in LIBH2. All possible historical events are listed and their direction of passage/distance from the blue hole site. The SLOSH simulated storm surges are also listed. The final column indicates which event most likely left each deposit.

Event Bed	Age range	Median Age	Historical events	Within 75 km?	Direction	Simulated storm surge (m)	Most Probable Event
EB 1	2011-2016	2014	Joaquin 2015 (Cat 4)	X	East	0.7	Joaquin 2015 (Cat 4)
			Sandy 2012 (Cat 2)	X	West	0.85	
			Irene 2011 (Cat 3)	X	East	0.94	
EB 2	1996-2015	2008	Sandy 2012 (Cat 2)	X	West	0.85	Irene 2011 (Cat 3)
			Irene 2011 (Cat 3)	X	East	0.94	
			Lili 1996 (Cat 2)	X	North	1.1	
			Erin 1995 (Cat 1)	X	East	0.43	
EB 3	1982-2014	2003	Sandy 2012 (Cat 2)	X	West	0.85	Lili 1996 (Cat 2)
			Irene 2011 (Cat 3)	X	East	0.94	
			Lili 1996 (Cat 2)	X	North	1.1	
			Erin 1995 (Cat 1)	X	East	0.43	
EB 4	1903-1966	1933	July 1933 (Cat 1)		East	0.24	1932 (Cat 4)
			1932 (Cat 4)	X	South	0.46	
			1928 (Cat 4)	X	East	1.37	
			Sept. 1926 (Cat 4)	X	West	0.91	
			July 1926 (Cat 4)	X	East	1.46	
			Nov. 1924 (Cat 1)		South	0.06	
			Sept. 1923 (Cat 1)	X	East	0.4	
EB 5	1900-1963	1929	July 1933 (Cat 1)		East	0.24	1928 (Cat 4)
			1932 (Cat 4)	X	South	0.46	
			1928 (Cat 4)	X	East	1.37	
			Sept. 1926 (Cat 4)	X	West	0.91	
			July 1926 (Cat 4)	X	East	1.46	
			Nov. 1924 (Cat 1)		South	0.06	
			Sept. 1923 (Cat 1)	X	East	0.4	
EB 6	1898-1962	1927	July 1933 (Cat 1)		East	0.24	July 1926 (Cat 4) Sept. 1926 (Cat 4)
			1932 (Cat 4)	X	South	0.46	
			1928 (Cat 4)	X	East	1.37	
			Sept. 1926 (Cat 4)	X	West	0.91	
			July 1926 (Cat 4)	X	East	1.46	

			Nov. 1924 (Cat 1)		South	0.06	
			Sept. 1923 (Cat 1)	X	East	0.4	
EB 7	1848-1916	1877	1852 (Cat 1)		East	0.24	1891 (Cat 2) 1866 (Cat 4)
			1866 (Cat 4)	X	West	0.73	
			1871 (Cat 2)		East	0.43	
			1882 (Cat 1)		South	0.21	
			1884 (Cat 1)	X	East	0.43	
			1891 (Cat 2)	X	East	0.76	
			1899 (Cat 3)		Southwest	0.3	